PCCP

Accepted Manuscript

This is an *Accepted Manuscript*, which has been through the Royal Society of Chemistry peer review process and has been accepted for publication.

Accepted Manuscripts are published online shortly after acceptance, before technical editing, formatting and proof reading. Using this free service, authors can make their results available to the community, in citable form, before we publish the edited article. We will replace this *Accepted Manuscript* with the edited and formatted *Advance Article* as soon as it is available.

You can find more information about *Accepted Manuscripts* in the Information for Authors.

Please note that technical editing may introduce minor changes to the text and/or graphics, which may alter content. The journal's standard Terms & Conditions and the Ethical guidelines still apply. In no event shall the Royal Society of Chemistry be held responsible for any errors or omissions in this *Accepted Manuscript* or any consequences arising from the use of any information it contains.

Intermolecular Bonding of Hemin in Solution and in Solid State Probed by N K-edge X-ray Spectroscopies

Ronny Golnak,[a,b] Jie Xiao,*[a] Kaan Atak,[a,c] Joanna S. Stevens,[d] Adrian Gainar,[d] Sven L. M. Schroeder,[e,f] Emad F. Aziz*[a,c]

a. Joint Ultrafast Dynamics Lab in Solutions and at Interfaces (JULiq), Institute of Methods for Material Development, Helmholtz-Zentrum Berlin für Materialien und Energie, Albert-Einstein-Strasse 15, D-12489 Berlin, Germany
b. Fachbereich Chemie, Freie Universität Berlin, Takustrasse 3, D-14195 Berlin, Germany
c. Fachbereich Physik, Freie Universität Berlin, Arnimallee 14, D-14195 Berlin, Germany
d. School of Chemical Engineering and Analytical Science, School of Chemistry, The University of Manchester, Oxford Road, Manchester M13 9PL, United Kingdom
e. School of Chemical and Process Engineering, University of Leeds, Leeds LS2 9JT, UK
f. DIAMOND Light Source Ltd., Harwell Science and Innovation Campus, Chilton, Didcot OX11 0DE, UK

*corresponding author: jie.xiao@helmholtz-berlin.de; emad.aziz@helmholtz-berlin.de

Abstract

X-ray absorption/emission spectroscopy (XAS/XES) at the N K-edge of iron protoporphyrin IX chloride (FePPIX-Cl, or hemin) has been carried out for dissolved monomers in DMSO, dimers in water and for the solid state. This sequence of samples permits identification of characteristic spectral features associated with the hemin intermolecular bonding. These characteristic features are further analyzed and understood at the molecular orbital (MO) level based on the DFT calculations.

Introduction

Metalloporphyrins are functional materials with extensive applications in catalysis, solar energy conversion and biological systems.[1–5] In these systems, porphyrin molecules are often in a solution environment, in which self-association can lead to different types of non-monomeric species. The differences in solvation and solute-solute interactions will consequently affect the functionality of metalloporphyrins, requiring studies of speciation in solution to further our understanding of their functionality. For example, iron protoporphyrin IX chloride (FePPIX-Cl, or hemin, Figure 1a) forms monomer species when dissolved in dimethyl sulfoxide (DMSO), while dimer structures are present in aqueous solution.[6–9] It is known that the electronic structure of hemin, especially the local electronic structure at the Fe center, which often serves as the major functional site, is altered due to dimerization.[7] Hemin oligomer species in various solvents have therefore been investigated previously by UV-Vis spectroscopy and X-ray absorption/emission spectroscopy (XAS/XES) at the Fe L-edge,[6–9] although the nature of the probed electronic transitions implied that the hemin intermolecular bonding interactions were probed rather indirectly. UV-Vis measures overlapping valence excitations of all components in the hemin solution, without differentiation between contributions from solute, solvent or solute-solvent interactions. The lack of exclusive probing of the π-π interactions expected for hemin dimerization left some ambiguity in the interpretation of the UV-Vis data.[9] XAS/XES measurements at the Fe L-edge, on the other hand, represent a local probe sensitive to the electronic structure changes at the Fe sites induced by hemin dimerization.[7] However, the information obtained for the dimerization is still fairly indirect, since hemin dimerization is primarily driven by π-π stacking of porphyrin rings, without intermolecular bonding by the Fe center, as illustrated in Figure 1b.[7–9] The characteristic L-edge features at the Fe sites[7] do of course depend on their interaction with the N moieties of the porphyrin ring, but the Fe center in hemin is also coordinated by a chloride ligand. Moreover, there is a sixth vacant coordination site perpendicular to the porphyrin plane, available for possible coordination by molecules from the solvent. Even though contributions of Fe-solvent interaction have been determined to be insignificant,[7] they cannot be completely excluded. It is therefore

2

difficult to unravel the different types of interactions at the Fe site for obtaining unambiguous information about the π-π interactions underlying dimerization.

Locally probing the N valence orbitals is expected to be a more explicit way of probing hemin dimerization, or the extent of hemin intermolecular interactions in general. The N moieties are part of the porphyrin ring and thus part of the valence system directly involved in the π-π stacking. Each N atom embedded in the porphyrin ring is fully coordinated with the metal center and C atoms of the porphyrin and consequently there is much less scope for strong interaction with solvent molecules. We have therefore targeted the local electronic structure at the N moieties through X-ray absorption/emission spectroscopy (XAS/XES), to obtain electronic structure information about the unoccupied and occupied valence states of hemin in solution.[5,10,11] We will show that solvent-dependent XA/XE spectral differences at the N K-edge are observable, and certain XA features are identified as spectral characteristics associated with the extent of hemin intermolecular bonding.

DMSO and 0.5 M NaOH aqueous solution were chosen as solvents to dissolve hemin powder as in previous studies. These solutions contain hemin monomer and dimer species, respectively.[6,7] The high pH value (from NaOH) of the aqueous solution increases hemin solubility in water, but adds potential additional complexity due to formation of the carboxylate anionic form in basic solution, as shown in Figure 1c. However, because the carboxylate groups are not conjugated with the π system of the porphyrin ring their influence on the N K-edge is expected to be minor, in contrast to the recently presented N K-edge spectra of para-aminobenzoic acid in solution, where the amine nitrogen felt the direct influence of the carboxylate group as both were part of the delocalised π system of the aromatic ring.[12]

Experimental Methods

Hemin (iron protoporphyrin IX chloride, FePPIX-Cl) powder from bovine (purity > 90%) was purchased from Sigma-Aldrich, and further dissolved in 0.5 M NaOH aqueous solution and dimethyl sulfoxide (DMSO) solvent to make 0.1 M and 0.05 M hemin solutions, respectively. The hemin solutions were introduced into a vacuum chamber by liquid micro-jet technique for the X-ray measurements.[13,14] Possible sample damage by

intense X-ray beam was effectively avoided since the liquid sample was constantly refreshed. The solid powders were spread across a double-sided adhesive copper tape attached to a copper plate which was mounted at 45° with respect to the incident photon beam in the vacuum chamber. The possible radiation damage to the solid samples was minimized by reducing incident photon flux and frequent changing of the measurement spots.

The experiment was carried out at the U41-PGM undulator beamline and LiXEdrom endstation at the synchrotron facility BESSY II, Berlin. The U41-PGM provides horizontally linear polarized light with high photon flux ($\sim 10^{13}$ photon/s) and small focal spot ($\sim$ 40 μm of vertical size), which is crucial to our measurements. High flux is required for low-concentration samples. Small vertical focal size ($\sim$ 40 μm) assures high energy resolution for XES measurements. The photons emitted from the sample were collected along the polarization direction of the incident photon beam (to suppress the elastic peak) and subsequently dispersed by a spherical grating with 1200 lines/mm and 7.5 m radius. The dispersed photons were then detected by a microchannel plate (MCP)/fluorescence screen/CCD assembly. The sample (micro-jet), grating, and photon detector are arranged in a Rowland circle geometry for accurate focusing. The grating and detector chamber was kept at a pressure of 10^{-8} mbar or lower to protect the grating and MCP surfaces from contamination, while the sample chamber was at 10^{-5} mbar. The incident photon energy was tuned to the N K-edge, and the N 2p → 1s transition was selected for the detection of the emitted photon from both liquid and solid samples, giving rise to the XE spectra. Integration of a series of XE spectra acquired at various excitation photon energies over the emitted photon energy delivers one XA spectrum, which is referred as XAS in partial-fluorescence-yield (PFY) mode.

Theoretical Calculations

The DFT calculations were conducted with the ORCA program package[15] to obtain the molecular orbital (MO) information of the hemin molecule in gas phase in the ground state.[6] Molecular geometry optimization was performed using the B3LYP DFT method together with the def2-TZVP(-f) basis set.[16–18] The N contributions to both occupied and unoccupied valence MO are acquired from Löwdin population analysis based on the DFT

calculations.[19] A Gaussian-type broadening of 0.5 eV with the respective weight (according to the N contribution) is applied to each valence MO and then summed up, to simulate the XA/XE spectra obtained at the N K-edge.

Results and Discussion

The obtained PFY-XA and XE spectra of hemin in DMSO (monomer) and in 0.5 M NaOH aqueous solution (dimer) are shown in Figure 2 as blue and red traces, respectively, along with the difference plot (black trace in the left panel) obtained from the subtraction of the monomer XA spectrum (blue) from that of the dimer (red). The XA spectra of the two hemin oligomer species are very similar but on closer inspection three regions with significant spectral differences can be identified, indicated by the three color-highlighted areas of the difference plot. The intense absorption feature at 398.5 eV, which represents the lowest unoccupied molecular orbital (LUMO) at the N sites, is associated with the porphyrin nitrogen in a N–Fe environment.[20,21] Such a low-lying energy feature is, therefore, completely absent in small metal-free N-containing molecules.[12,22,23] The metal-free porphyrin (2HTPP) usually has the first N absorption feature located more than 1 eV below the metal-N peak with much reduced intensity, arising from the inequivalence of the N species in the absence of the metal centre, leading to iminic =N− and pyrrolic −NH− nitrogen.[20,21] The slight energy shift between the two absorption edges at around 398 eV is made evident by the blue-highlighted area in the difference plot, which actually indicates a broadening, instead of an energy shift, of the first absorption feature for the hemin dimer species since its peak position at 398.5 eV does not exhibit observable shift when compared with that of hemin monomer (the broadening effect is discussed below). Nonetheless, the N–Fe features of the two hemin species are in general very similar, which is in line with the similarity of the LUMO observed in the Fe L-edge XA spectra,[7] indicating that the N–Fe bonding is not strongly influenced by the dimerization process, or affected by the different solvents significantly. The absorption features at 400-403 eV (green-highlighted) originate from N π^* orbitals as N is part of the aromatic ring system, while the arising absorption edges at the brown-highlighted area are in the region of the ionization potentials (IPs).[12,22] The N π^* orbitals

and IP thus exhibit distinguishable characteristics for different hemin solutions. The exact origins of these differences will be discussed in detail for Figure 3 below.

Besides the unoccupied valence orbitals revealed by XAS, slight differences between the occupied valence states at the N sites are also uncovered by the XE spectra of the two hemin solutions (Figure 2). Emitted photon energies, instead of photon energy losses that are often observed in highly localized and correlated electron systems as in d or f orbitals, are shared by the N XE features measured at various excitation energies, marked by vertical dashed green lines in Figure 2. The absence of the loss features indicates little electron correlation in the N 2p orbitals, as expected for generally delocalized orbitals like valence s or p. The XE spectra of hemin in NaOH aqueous solution (red traces) present generally a better resolution (narrower peaks) when compared with the spectra of hemin in DMSO (blue traces). This is in line with the previous observation at the Fe L-edge that the Fe XE peaks of hemin dimer species are narrower than those of hemin monomer, owing to the higher degree of orbital localization induced by hemin dimerization.[7] Different degrees of orbital delocalization (or localization) in the two hemin oligomer species also lead to the elastic peaks with different intensities. The elastic peak of each red XE spectrum (hemin dimer) in Figure 2 shows higher intensity than the blue trace (hemin monomer) when the excitation energy tuned to the corresponding absorption peaks, indicating higher cross-sections of the N 2p → 1s transition for hemin dimer. It can be argued that the higher degree of orbital localization in hemin dimer preserves a density of states (DOS) with the p character of the N 2p orbital better than in the hemin monomer, resulting in more dipole-allowed 2p → 1s transitions. If the N 2p orbitals mixes more with Fe 3d orbitals, lower transition probability is expected since lower DOS with p character is present at the N sites due to the higher extent of N 2p orbital delocalization in the hemin monomer.

The more intense elastic peak and better resolved emission features in the N XE spectra of hemin in aqueous solution could be regarded as an indicator of hemin dimerization, similar to the observation of the local energy gap opening at the Fe L-edge used to indicate the hemin dimerization.[7] However, unlike the local gap opening at the Fe L-edge that involves the energy shift of the characteristic spectral feature, these observed spectral differences in the N XE spectra only contain intensity variations. Signal

strength often largely depends on extrinsic parameters and thus cannot be used as an intrinsic and reliable indicator for hemin dimerization. The observed differences of the N π^* orbitals and IP (green and brown areas) in the N XA spectra in Figure 2 may, however, intrinsically differentiate between hemin monomer and dimer species. It is instructive to compare these N XA spectra of the small scale intermolecular bonding species (dimer) in Figure 2 with that of a large scale case in solid form, to clearly identify the characteristic spectral evolution under the various extents of hemin aggregation. Such a comparison of the XA spectra is presented in Figure 3, with their respective fitted components (green traces) as well as the summations of the components (red traces). Each individual fitted Gaussian component below IP is marked by vertical dashed lines and labeled as A, B, C, D and E. The IPs are fitted by *arctan* step functions with their energy positions marked by vertical lines as well.

The most striking difference between the solid state and the solution spectra is the considerable broadening of almost all the spectral features in the solid state spectrum. This is likely due to the extensive orbital overlapping in the solid state [24,25] and was also somewhat evident in the previous study of aminobenzoic acid.[12] Self-absorption distortions of the spectrum from the more dense solid state may also contribute to the observed broadening of features. This solid state broadening makes the component A, originating from the N–Fe interaction as discussed in Figure 2, and component B resolvable in Figure 3a and 3b after the Gaussian fitting appear to be irresolvable in Figure 3c. The feature B may stem from a multi-electron excitation, *e.g.* a shake-up satellite to feature A, or reflect an electronic state that originates from solute-solvent interactions since the ground state calculation (vertical bars at the bottom of Figure 4) does not give rise to any molecular orbitals in this energy region. Feature A keeps relatively similar peak widths in Figures 3a and 3b because the N–Fe interaction is not directly involved in the dimerization process. However, its broadening in Figure 3c suggests that the hemin oligomer species in the solid form may adopt different forms of intermolecular bonding that may involve the N–Fe interaction to some extent. Components C and D, constituting the green-highlighted difference in Figure 2, exhibit monotonic energy shifts from the monomer (Figure 3a) to the dimer (3b), and appear to be even lower in the solid (3c). It seems that these features are associated with the

development of hemin-hemin interactions and can therefore be used to characterize the extent of intermolecular bonding. The shifts of the features C and D to lower energies indicate that the measured energy level distances between the N π^* orbitals and the N 1s core level are systematically reduced when a larger scale of the hemin oligomer species is realized. The origin of this energy shift could be either an initial state effect in that either the valence N π^* orbitals are lowered or the N 1s core level binding energy raised. Alternatively, a final state effect may contribute, perhaps reflecting differences in valence charge relaxation upon core-hole formation, analog to the relaxation shift of CO molecules going from gas phase to solid state observed in photoelectron spectroscopy.[26] However, recent studies of bipyridine acid salts and co-crystals indicated that the effect of final state effects on the relative positions of π^* features are negligible, even when comparing bipyridine nitrogen species in very different local chemical environments.[27] Further inspection into the individual components C and D uncovers that the feature C remains roughly constant in peak width from Figure 3a to 3c, while the feature D becomes broader and relatively more intense upon hemin aggregation. The mechanism of this distinct peak evolution is likely due to the different extents of the orbital involvement in the hemin intermolecular bonding interactions which will be discussed in detail for Figure 4 based on a molecular orbital (MO) picture derived from DFT calculations.

The evolution of feature E is very similar to feature A, both exhibiting solid state broadening. However, the feature E does not have a sole MO origin as for feature A where the N–Fe interaction can be assigned, because it consists of contributions of many MOs. A similar situation also occurs for the broadest fitted Gaussian components with their centers located above the IPs, representing contributions from a number of MOs, as illustrated by the vertical bars at about 404-411 eV at the bottom of Figure 4. Strictly speaking, each spectral feature in Figure 3 comprises multiple MOs, and therefore should not be represented by a single Gaussian function in principle. Nevertheless, the fittings of the components A, B, C and D with a single Gaussian function still hold the physical significance discussed above because the contributed MOs to each component are very few in number and also located closely to each other in energy, as demonstrated in Figure 4. The characteristic spectral features that can distinguish various hemin oligomer species

are therefore the features C and D in Figure 3 exhibiting systematic energy shifts, and consequently associated with the extent of hemin intermolecular interactions.

The energy shifts of the IPs, however, do not follow the monotonic energy shift when going from dimer to solid, as shown in Figure 3b and 3c. The IP shift from Figure 3a to 3b is in line with the energy shift of the features C and D, which seems to suggest they have the same origin – elevation of the N 1s level. However, the core level argument cannot explain the non-shifting features, such as feature A, and the opposite shifting of the IP in the spectrum of the solid sample. The other mechanism discussed above, *i.e.* the initial state effect of the valence orbital shifting, has to come to play.

With the help of the ground state DFT calculations, the origins of the characteristic features C and D that exhibit distinct spectral evolutions of the component width and intensity in Figure 3 is uncovered at a MO level. The theoretically simulated spectrum at the occupied and unoccupied valence levels, obtained from the summation of individual N contributions with a universal Gaussian broadening, is plotted in Figure 4, along with the combined XA and XE spectra of the hemin monomer (in DMSO) and dimer (in NaOH aqueous solution) for comparison. The N contribution to each calculated MO, shown as vertical bars at the bottom of Figure 4, is acquired from the Löwdin population analysis based on the DFT calculations of the gas phase hemin in the ground state. Even though the experimental spectra are acquired from the core-hole excited final state (XAS) or initial state (XES), the simulated peak positions from the ground state calculation are in good agreement with experiment, allowing for accurate and reliable assignments of the calculated MOs to the experimental peaks. The characteristic features C and D in Figure 3 can therefore be visualized as the MOs presented in Figure 4. As illustrated in Figure 4, the feature C mainly originates from the orbitals localized at a single N atom; while the feature D, on the other hand, is from the orbitals delocalized over all four N atoms, as highlighted by dotted green circles. With development of the hemin intermolecular bonding through π-π stacking of the porphyrin ring, the feature D that involves four N atoms will surely develop a higher extent of the peak width broadening as well as intensity enhancement, owing to the extensive orbital overlapping, when compared with the feature C that has only very localized orbitals involved in the hemin-hemin interaction. The localized nature of the feature C inhibits its orbital

overlapping with neighbor orbitals and consequently suppresses the broadening and enhancement of the fitted peak, as demonstrated in Figure 3.

Due to the computational challenges for large-scale hemin oligomer species – dimer and above – the DFT calculations are only performed on a geometry-optimized isolated hemin monomer. The proposed N 1s core level shift arising from the different hemin oligomer species is therefore unable to be probed. The DFT calculations are carried out on the ground state, so that the final state effect is not possible to investigate. The spectrum of the solid sample is not included in Figure 4 for the comparison with the theoretical simulation because the strong solid state effect is expected to have significant influences on both initial state shifting and final state relaxation, which shifts certain experimental peaks significantly when compared with those of the isolated molecules, as has been demonstrated in Figure 3 for the features C and D. Therefore, attempted assignments of the calculated MOs performed on the gas phase molecules to the solid state features may not possess high credibility.

Conclusions

X-ray absorption and emission spectroscopy (XAS/XES) have been performed on solvated hemin molecules dissolved in DMSO and NaOH aqueous solution, as well as on the solid state. Characteristic features in the N XA spectra are identified and associated with electronic structure changes arising from hemin intermolecular bonding interactions. The spectral evolutions of these features upon the development of hemin-hemin interactions are further analyzed at the molecular orbital level derived from the DFT calculations. The results show that N K-edge X-ray spectroscopies provide experimental access to porphyrin intermolecular interactions in solution and in the solid state by tracking the energy shifts of the characteristic N K-edge XA features, crucially permitting *in situ* detection for electronic structure investigations. The exact energy positions of these characteristic features also provide a reference to help identify hemin oligomer species in solution, *e.g.* monomer in DMSO or dimer in aqueous solution.

Acknowledgements

References

[1] M. Ethirajan, Y. Chen, P. Joshi, R. K. Pandey, *Chem. Soc. Rev.* **2010**, *40*, 340–362.

[2] D. González-Rodríguez, G. Bottari, *J. Porphyr. Phthalocyanines* **2009**, *13*, 624–636.

[3] L.-L. Li, E. W.-G. Diau, *Chem. Soc. Rev.* **2012**, *42*, 291–304.

[4] A. Vecchi, P. Galloni, B. Floris, V. N. Nemykin, *J. Porphyr. Phthalocyanines* **2013**, *17*, 165–196.

[5] E. F. Aziz, *J. Phys. Chem. Lett.* **2011**, *2*, 320–326.

[6] K. Atak, R. Golnak, J. Xiao, E. Suljoti, M. Pflueger, T. Brandenburg, B. Winter, E. F. Aziz, *J. Phys. Chem. B* **2014**, *118*, 9938–9943.

[7] R. Golnak, J. Xiao, K. Atak, M. Khan, E. Suljoti, E. F. Aziz, *J. Phys. Chem. B* **2015**, *119*, 3058–3062.

[8] A. C. Maehly, å. Åkeson, G. Bergson, A. Grönvall, B. Zaar, E. Diczfalusy, *Acta Chem. Scand.* **1958**, *12*, 1259–1273.

[9] K. A. de Villiers, C. H. Kaschula, T. J. Egan, H. M. Marques, *JBIC J. Biol. Inorg. Chem.* **2007**, *12*, 101–117.

[10] K. M. Lange, E. F. Aziz, *Chem. Soc. Rev.* **2013**, *42*, 6840–6859.

[11] E. Suljoti, R. Garcia-Diez, S. I. Bokarev, K. M. Lange, R. Schoch, B. Dierker, M. Dantz, K. Yamamoto, N. Engel, K. Atak, et al., *Angew. Chem. Int. Ed.* **2013**, *52*, 9841–9844.

[12] J. S. Stevens, A. Gainar, E. Suljoti, J. Xiao, R. Golnak, E. F. Aziz, S. L. M. Schroeder, *Chem. – Eur. J.* **2015**, *21*, 7256–7263.

[13] K. M. Lange, R. Könnecke, S. Ghadimi, R. Golnak, M. A. Soldatov, K. F. Hodeck, A. Soldatov, E. F. Aziz, *Chem. Phys.* **2010**, *377*, 1–5.

Physical Chemistry Chemical Physics Accepted Manuscript

[14]   R. Golnak, K. Atak, E. Suljoti, K. F. Hodeck, K. M. Lange, M. A. Soldatov, N. Engel, E. F. Aziz, *Phys. Chem. Chem. Phys.* **2013**, *15*, 8046–8049.

[15]   F. Neese, *Wiley Interdiscip. Rev. Comput. Mol. Sci.* **2012**, *2*, 73–78.

[16]   A. D. Becke, *Phys. Rev. A* **1988**, *38*, 3098–3100.

[17]   A. D. Becke, *J. Chem. Phys.* **1993**, *98*, 5648–5652.

[18]   F. Weigend, R. Ahlrichs, *Phys. Chem. Chem. Phys.* **2005**, *7*, 3297–3305.

[19]   K. Atak, R. Golnak, J. Xiao, M. Pflüger, T. Brandenburg, B. Winter, E. F. Aziz, *Phys. Chem. Chem. Phys.* **2015**, *17*, 3409–3414.

[20]   M. V. Nardi, R. Verucchi, L. Pasquali, A. Giglia, G. Fronzoni, M. Sambi, G. Mangione, M. Casarin, *Phys. Chem. Chem. Phys.* **2015**, *17*, 2001–2011.

[21]   N. Schmidt, R. Fink, W. Hieringer, *J. Chem. Phys.* **2010**, *133*, 054703.

[22]   J. S. Stevens, C. R. Seabourne, C. Jaye, D. A. Fischer, A. J. Scott, S. L. M. Schroeder, *J. Phys. Chem. B* **2014**, *118*, 12121–12129.

[23]   M. J. Thomason, C. R. Seabourne, B. M. Sattelle, G. A. Hembury, J. S. Stevens, A. J. Scott, E. F. Aziz, S. L. M. Schroeder, *Faraday Discuss.* **2015**, *179*, 269–289.

[24]   J. Xiao, P. A. Dowben, *J. Phys. Condens. Matter* **2009**, *21*, 052001.

[25]   J. Xiao, P. A. Dowben, *J. Mater. Chem.* **2009**, *19*, 2172–2178.

[26]   H.-J. Freund, M. Neumann, *Appl. Phys. A* **1988**, *47*, 3–23.

[27]   J. S. Stevens, L. K. Newton, C. Jaye, C. A. Muryn, D. A. Fischer, S. L. M. Schroeder, *Crystal Growth & Design* **2015**, *15,* 1776–1783.
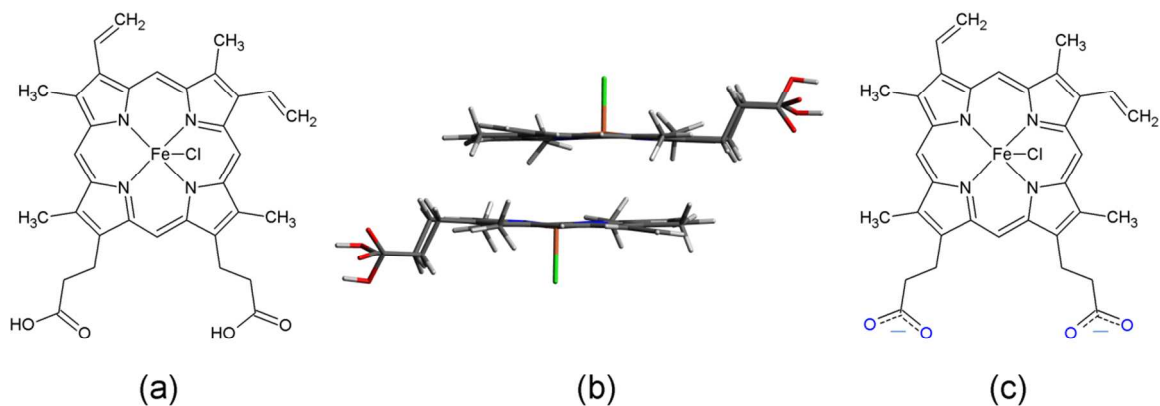
Figure 1. (a) Schematic of hemin chemical structure with neutral carboxyl groups (COOH), (b) geometrical arrangement of hemin dimer, and (c) schematic of hemin chemical structure with anionic carboxylate groups (COO⁻).
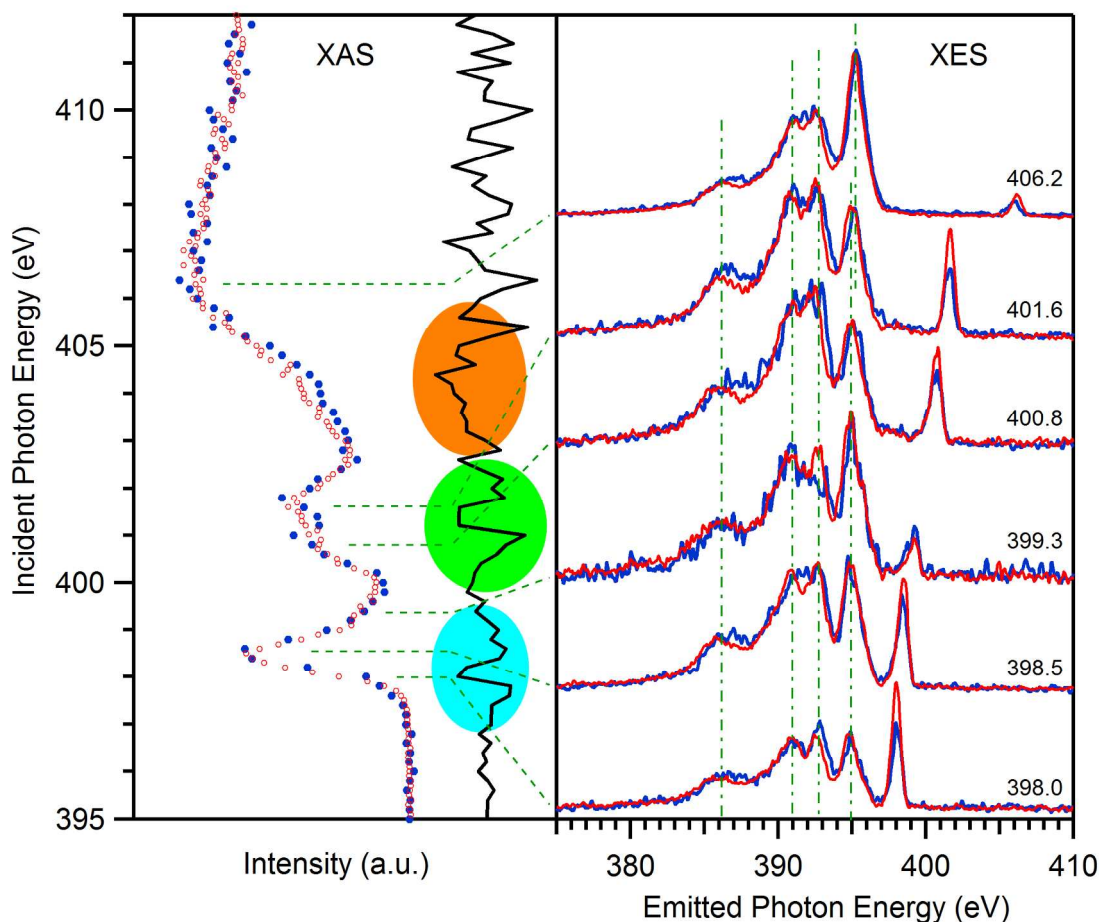
Figure 2. PFY-XA and XE spectra of hemin dissolved in DMSO (blue) and in NaOH aqueous solution (red). The black trace is the difference plot of the two XA spectra, with color-highlighted areas indicating the differences observed in the PFY-XA spectra of the two hemin solutions. The excitation energies used for XES measurements are labeled on the right side of the figure, and also indicated by horizontal green dashed lines pointing to the corresponding PFY features in the left panel. The vertical green dashed lines in the right panel mark the major XE features at the N K-edge. All spectra were normalized to their respective background for intensity comparison.
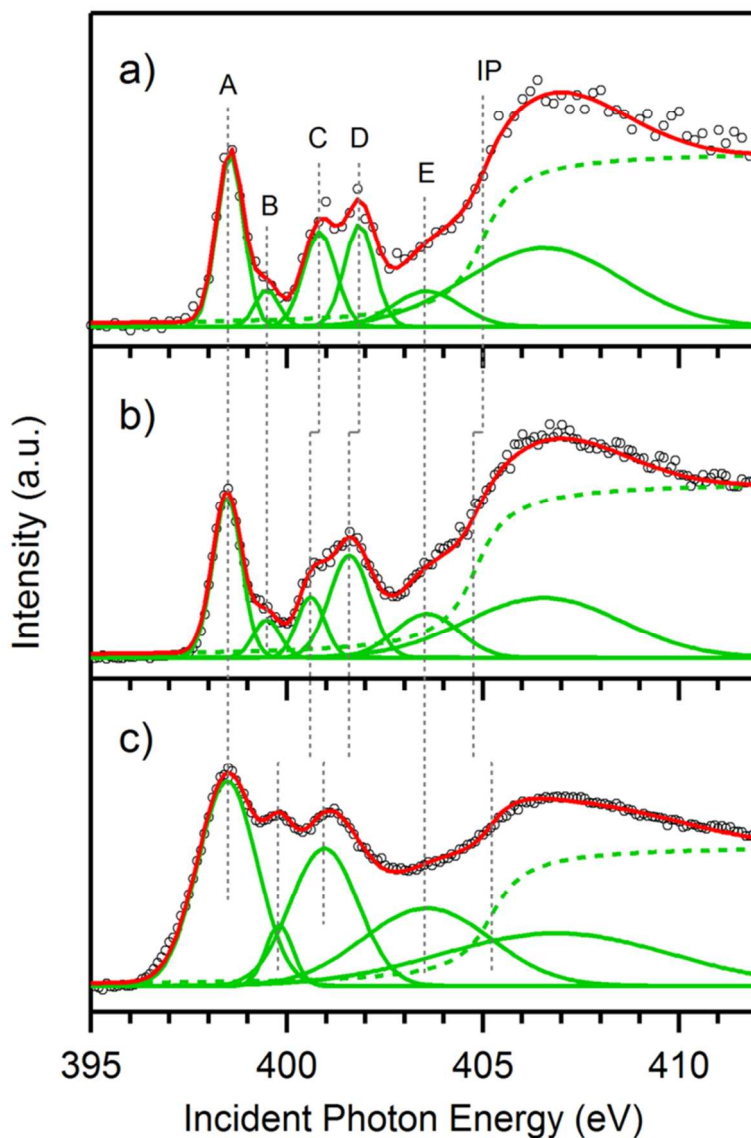
Figure 3. N K-edge PFY-XA spectra, represented by circles ○, of a) hemin in DMSO, b) hemin in NaOH aqueous solution and c) hemin powder in solid form, with their respective fitted components in green and the summation of these components in red. The ionization potential (IP) is fitted by step functions *arctan*, represented as green dashed traces, while the other components by Gaussian functions (solid green traces) with labels A, B, C, D and E. The energy positions of the IP and fitted Gaussian components, as well as their relative energy offsets, are marked by grey dashed lines.
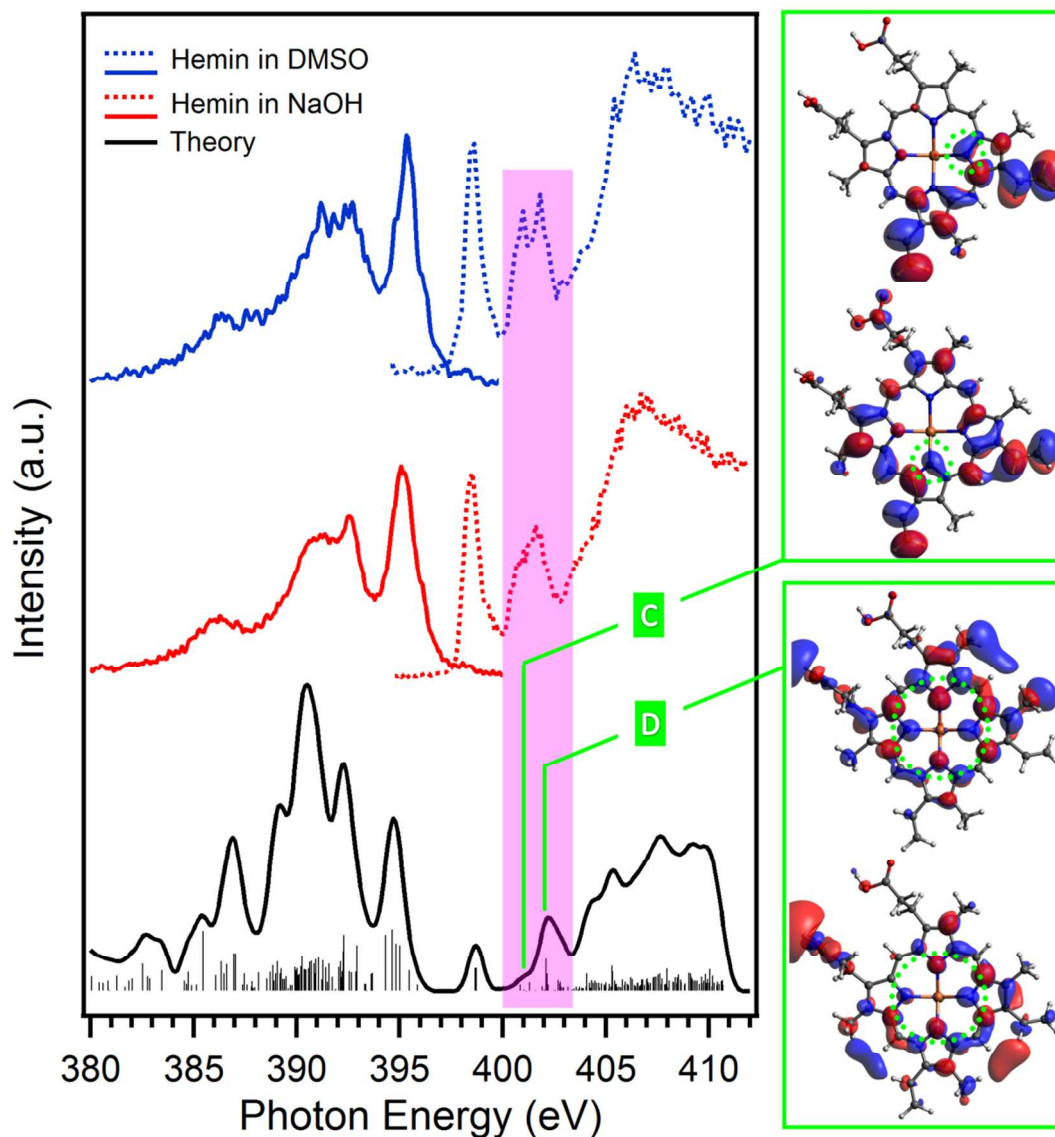
Figure 4. Off-resonant XE spectra (solid blue and red traces) at the excitation energies of 420 eV for the hemin dissolved in DMSO and NaOH aqueous solution, respectively, combined with their respective PFY-XA spectra (dashed blue and red traces). The experimental spectra are identical to the corresponding spectra in Figure 2. The theoretical DFT calculations and individual MOs weighted by N contributions are shown at the bottom as black trace and vertical bars, respectively. The characteristic features C and D identified in Figure 3 are assigned to certain calculated MOs with visualized orbitals presented on the right side of the figure. The orbitals localized at the N sites are highlighted with dotted green circles.

TOC Figure
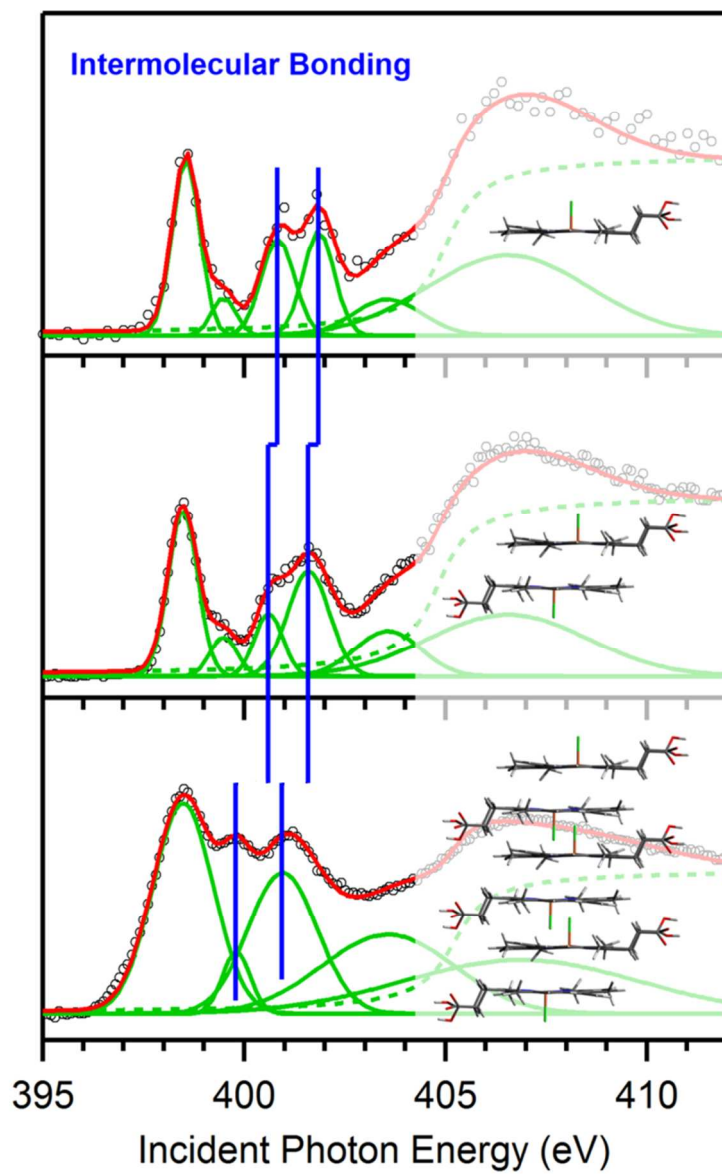
Characteristic X-ray absorption features indicate the extent of hemin intermolecular bonding interaction.